IOSR Journal of Mathematics (IOSR-JM)
e-ISSN: 2278-5728, p-ISSN: 2319-765X. Volume 19, Issue 3 Ser. 2 (May. – June. 2023), PP 20-31
www.iosrjournals.org

Numerical Investigation Of Heat And Mass Transfer In Hydromagnetic Williamson Nanofluids Flow Over Porous Exponentially Stretching Sheet With Heat Generation/Absorption And Thermal Radiation.

Kapil Kumar[1,] Bhupander singh[2], Pravendra Kumar[3]
Research Scholar, Department of Mathematics, Meerut College, Meerut
Professor, Department of Mathematics, Meerut College, Meerut
Research Scholar, Department of Mathematics, Meerut College, Meerut

Abstract:
An analysis has been carried out to study a problem of the heat generation/absorption and thermal radiation effects on Heat and Mass transfer in Hydromagnetic Williamson nanofluids flow over an exponentially stretching sheet in porous medium. Using appropriate similarity transformations, the governing nonlinear partial differential equations are transformed into non-linear ordinary differential equations. The transformed non-linear ordinary differential equations are then solved numerically by in built bvp4c solver package in MATLAB. The velocity profile, temperature profile and concentration profile are discussed and the influence parameters like Brownian motion parameter, Thermophoresis parameter, Thermal radiation parameter, Prandtl number, Heat source/sink parameter, Williamson parameter, Porosity parameter, Hartmann number and Lewis number are depicted graphically.

Keywords: *Nanofluids, Williamson fluid, Hydromagnetic, Heat generation/absorption, Thermal Radiation, Exponentially stretching sheet.*

Date of Submission: 28-05-2023 Date of Acceptance: 08-06-2023

I. Introduction

Nanofluids studies have attracted on considerable attention of researchers due to many industrial and technological application that includes both metal and polymer sheets. Because of its importance in industrial processing of glass fibre, metal wires, polymer sheets, paper production, and plastic films, the evaluation of heat transfer across a boundary layer flow through a continuous stretched surface subject to the prescribed heat flux and surface temperature has piqued interest. In the manufacturing of plastic and glass, the pace of cooling is significantly reliant on the feature of the finished product. Sakiadis [1] investigated the flow of the boundary layer across a continuous stretched surface by developing two-dimensional boundary layer equations. Tsou et al. [2] investigated the heat transfer across a boundary layer flow subjected to a stretched surface. Erickson et al. [3] expanded on this work to examine mass transfer in the context of suction and injection. The flow of boundary layer across a linear stretched surface has also studied by the researcher [4, 5, 6]. Norfifah et al [7] investigated the steady boundary-layer flow of a nanofluid past a moving semi-infinite flat plate in a uniform free stream. The found that dual solutions exist when the plate and the free stream move in the opposite directions. The dual solution for the flow of hybrid nanofluid assuming the existence of mixed convection along a curved stretching/shrinking surface determined by Khan M. R. et al. [8]. With the influence of mass suction on the oscillatory surface, Nadeem et al. [9] examined an unsteady magnetohydrodynamic oblique stagnation point flow of an incompressible nanofluid towards a stretching/shrinking surface.

A nanofluid is a fluid that contains nanoparticles, which are usually metals or metal oxides. Nanoparticles have a large surface area and stability. Choi [10] was the first who introduce the term “nanofluid”. In addition to heat transfer performance, nanoparticles enhanced the thermophysical phenomenon. Heat transfer efficiency is influenced by nanoparticle material type, shape, and dispersed particle and so on. In nanofluids, Brownian diffusion and thermophoresis are necessary slip mechanics. Buongiorno [11] constructed a mathematical model of nanofluid that integrates thermophoresis and Brownian motion effects, utilising various physical parameters and attempting to control nanoparticles by assumption. The Cheng-Minkowycz problem of free convective flow in a permeable medium immersed by a nanofluid was solved by Nield and Kuznetsov [12], who used Buongiorno's model. Pal and Mandal [13] explored the flow of an electrically conducting MHD boundary layer of a nanofluid through a nonlinear stretching/shrinking surface with Ohmic heating, thermal radiation, and heat generation/absorption. For greater values of the heat generation/absorption parameter, they discovered the existence of dual solutions. Das [14] investigated the flow of nanofluid across a nonlinear stretching sheet while accounting for the surface temperature that was set in the presence of a partial condition effect. It was demonstrated that when nonlinear stretching sheet parameter and slip parameters increased, the velocity of the nanofluid decreased and the thickness of the boundary layer increased. Nasir et al. [15] presented the MHD flow and heat transfer of couple stress fluid past an oscillatory stretching sheet in the presence of heat source and sink embedded in porous medium. Non-Newtonian fluid is taken into account in the study of chemical reaction and the impact of thermal radiation on nanoparticles by Bhatti et al. [16]. There are two different sorts of non-Newtonian fluids: those that depend on time and those that do not. Williamson fluid is a pseudo-plastic, non-Newtonian fluid that is independent of time. In many manufacturing and engineering processes, including as the extraction of the surface of polymers and the production of photographic images, non-Newtonian nanofluid boundary flow across a linear surface is used. Discussing pseudoplastic materials and putting out a fluid model for non-Newtonian fluids, which came to be known by his name, were pioneering works by Williamson [17]. In 1929, this model was released. Due to its usefulness, this model has been utilised by several studies [18, 19, and 20] throughout the previous decade to illustrate the actual behaviour of fluids. Krishnamurthy et al. [21] studied numerically the impact of radiation and chemical reactions on the steady boundary layer flow of MHD Williamson fluid through porous medium toward a horizontal linearly extending sheet in the presence of nanoparticles. Williamson fluid two-dimensional flow analysis modelling across a linear and exponentially stretching surface was introduced by Nadeem et al. [22,23]. The series solution for the time independent MHD flow of Williamson fluid through a porous plate was carried out by Hayat et al. [24]. Williamson fluid has been studied in two dimensions across a stretching sheet by Nadeem and Hussain [25], who also examined the impact of nanoparticles on the fluid. Williamson nanofluid flow across an exponentially porous stretched surface was examined by Ahamed and Akbar [26] while taking two heat transfer cases into consideration. Additionally, some important recent research [27-39] on the flow of Williamson nanofluids have been conducted.

II. Mathematical formulation:

Take into account the steady Williamson nanofluid flow in two dimensions across a stretched porous exponential surface. It is assumed that the sheet is stretched along x-axis with the exponentially varying velocity U_w and y-direction is taken perpendicular to the sheet. Apply the magnetic field to the fluid flow perpendicularly and heat generation/absorption is considered. The fundamental equations of conservation of mass, momentum, energy, and concentration for the present problem can be written in Cartesian coordinates x and y as

$$\frac{\partial u}{\partial x}+\frac{\partial v}{\partial y}=0 \tag{1}$$

$$u\frac{\partial u}{\partial x}+v\frac{\partial u}{\partial y}=\nu\frac{\partial^2 u}{\partial y^2}+\sqrt{2}\nu\Gamma\frac{\partial u}{\partial y}\frac{\partial^2 u}{\partial y^2}-\nu\frac{u}{\kappa_1}-\frac{\sigma {B_0}^2}{\rho}u \tag{2}$$

$$u\frac{\partial T}{\partial x}+v\frac{\partial T}{\partial y}=\alpha\frac{\partial^2 T}{\partial y^2}+\frac{Q_0}{(\rho C_p)_f}(T-T_\infty)+\frac{(\rho C_p)p}{(\rho C_p)_f}\left[D_B\frac{\partial T}{\partial y}\frac{\partial C}{\partial y}+\frac{D_T}{T_\infty}\left(\frac{\partial T}{\partial y}\right)^2\right]-\frac{1}{(\rho C_p)}\frac{\partial q_r}{\partial y} \tag{3}$$

$$u\frac{\partial C}{\partial x}+v\frac{\partial C}{\partial y}=D_B\left(\frac{\partial^2 C}{\partial y^2}\right)+\frac{D_T}{T_\infty}\left(\frac{\partial^2 T}{\partial y^2}\right) \tag{4}$$

Where u is the velocity component along x direction and v is the velocity component along y direction, T is the temperature of nanofluid, ν is kinematic viscosity, σ is electric conductivity, ρ is the density, B_0 is the constant of strength magnetic field. The appropriate boundary conditions are given by

$$u=u_w=U_0 exp^{\left(\frac{x}{l}\right)},\quad v=0,\ T=T_w,\ C=C_w\quad at\ y=0 \tag{5}$$

$$u=u_e\to 0,\quad T=T_\infty,\quad C=C_\infty\quad as\quad y\to\infty \tag{6}$$

The radiative heat flux under Rosseland approximation for radiation is given by

$$q_r=-\frac{4\,\sigma^*}{3\,k^*}\frac{\partial T^4}{\partial y} \tag{7}$$

Where σ^* is the Stefan Boltzmann constant and k^* is the Rosseland mean absorption coefficient. It is further assumed that the temperature diffusion with in the flow are sufficiently small, we may expand the term T^4 due to radiation as a linear function of the temperature in Taylor series about T_∞ and can be approximated after neglecting the higher order terms as

$$T^4\approx 4{T_\infty}^3T-3{T_\infty}^4 \tag{8}$$

Using Eqs. (7) and (8), we obtain

$$\frac{\partial q_r}{\partial y}=-\frac{16\sigma^*{T_\infty}^3}{3\,k^*}\frac{\partial^2 T}{\partial y^2} \tag{9}$$

Using similarity transformation, the governing nonlinear partial differential equations are as transformed into system of ordinary differential equations defined by

$$\boldsymbol{u} = \boldsymbol{u_0}\, \boldsymbol{exp}^{\left(\frac{x}{l}\right)} \boldsymbol{f}'(\eta), \qquad \eta = \sqrt{\frac{\boldsymbol{u_0}}{\boldsymbol{2\nu l}}}\, \boldsymbol{y}\, \boldsymbol{exp}^{\left(\frac{x}{2l}\right)}, \qquad \boldsymbol{v} = -\sqrt{\frac{\boldsymbol{\nu\, u_0}}{\boldsymbol{2\, l}}}\, \boldsymbol{exp}^{\left(\frac{x}{2l}\right)} [\boldsymbol{f}(\eta) + \eta\, \boldsymbol{f}'(\eta)]$$

$$T = T_\infty + (T_w - T_\infty) exp^{\left(\frac{x}{2l}\right)} \Theta(\eta), \qquad \phi(\eta) = \frac{(C - C_\infty)}{(C_w - C_\infty)}$$

In view of the similarity transformation defined above, equation (1) satisfies in identical manner as well as equations (2), (3) and (4) are reduced to the subsequent set of nonlinear ODE's

$$\boldsymbol{f}'''(\eta) + \boldsymbol{f}(\eta)\boldsymbol{f}''(\eta) - \boldsymbol{2}(\boldsymbol{f}'(\eta))^2 + \boldsymbol{\lambda f}'''(\eta)\boldsymbol{f}''(\eta) - (\boldsymbol{K} + \boldsymbol{M})\boldsymbol{f}'(\eta) = \boldsymbol{0} \tag{10}$$

$$(\boldsymbol{1} + \boldsymbol{Nr})\Theta''(\eta) + \mathbf{Pr}[\Theta'(\eta)\boldsymbol{f}(\eta) - \boldsymbol{f}'(\eta)\Theta(\eta) + \boldsymbol{Q}\Theta(\eta) + \boldsymbol{N_b}\Theta'(\eta)\boldsymbol{\phi}'(\eta) + \boldsymbol{N_t}(\Theta')^2] = \boldsymbol{0} \tag{11}$$

$$\boldsymbol{\phi}''(\eta) + \boldsymbol{LePrf}(\eta)\boldsymbol{\phi}'(\eta) + \frac{\boldsymbol{N_t}}{\boldsymbol{N_b}}\Theta''(\eta) = \boldsymbol{0} \tag{12}$$

Subject to the following boundary conditions

$$\boldsymbol{f}(\boldsymbol{0}) = \boldsymbol{0}, \;\; \boldsymbol{f}'(\boldsymbol{0}) = \boldsymbol{1}, \;\; \Theta(\boldsymbol{0}) = \boldsymbol{1}, \;\; \boldsymbol{\phi}(\boldsymbol{0}) = \boldsymbol{1} \qquad \text{at } \eta = 0 \tag{13}$$

$$\boldsymbol{f}'(\infty) = \boldsymbol{0}, \;\; \Theta(\infty) = \boldsymbol{0}, \;\; \boldsymbol{\phi}(\infty) = \boldsymbol{0} \qquad \text{at } \eta \to \infty \tag{14}$$

The similarity parameters in above equations (10), (11) and (12) are $\boldsymbol{N_b}, \boldsymbol{N_t}, \boldsymbol{Nr}, \boldsymbol{Pr}, \boldsymbol{Q}, \boldsymbol{\lambda}, \boldsymbol{K}, \boldsymbol{M}$ and $\boldsymbol{Le}$ which respectively represents the Brownian motion parameter, Thermophoresis parameter, Thermal radiation parameter, Prandtl number, Heat source/sink parameter, Williamson parameter, Porosity parameter, Hartmann number and Lewis number. These parameters are defined as

$$\boldsymbol{N_b} = \boldsymbol{\tau}\frac{\boldsymbol{D_B(c_w - c_\infty)}}{\boldsymbol{\nu}}, \;\; \boldsymbol{N_t} = \boldsymbol{\tau}\frac{\boldsymbol{D_T(T_w - T_\infty)}}{\boldsymbol{T_\infty \nu}}\boldsymbol{e}^{x/2l}, \;\; \boldsymbol{Nr} = \frac{\boldsymbol{16}}{\boldsymbol{3}}\frac{\boldsymbol{\sigma^* T_\infty}^3}{\boldsymbol{k^* k_\infty}}, \;\; \boldsymbol{Pr} = \frac{\boldsymbol{\nu}}{\boldsymbol{\alpha}}, \boldsymbol{Q} = \frac{\boldsymbol{Q_0}}{(\boldsymbol{\rho c_P})_{\boldsymbol{f}}}\frac{\boldsymbol{2l}}{\boldsymbol{U_0}}\boldsymbol{e}^{-\frac{x}{l}}$$

$$\boldsymbol{\lambda} = \boldsymbol{\Gamma}\left(\frac{\boldsymbol{U_0}^3}{\boldsymbol{\nu l}}\right)^{1/2}\boldsymbol{e}^{3x/2l}, \boldsymbol{K} = \frac{\boldsymbol{2l}}{\boldsymbol{U_0}}\frac{\boldsymbol{\nu}}{\boldsymbol{\kappa_1}}\boldsymbol{e}^{-x/l}, \boldsymbol{M} = \frac{\boldsymbol{2l}}{\boldsymbol{U_0}}\frac{\boldsymbol{\sigma B_0}^2}{\boldsymbol{\rho}}\boldsymbol{e}^{-x/l}, \quad \boldsymbol{Le} = \frac{\boldsymbol{\alpha}}{\boldsymbol{D_B}} \tag{15}$$

The mathematical expressions for various physical quantities of interest like skin friction coefficient, local Nusselt number and the Sherwood number are defined as

$$\boldsymbol{C_f} = \frac{\boldsymbol{\tau_w}}{\boldsymbol{\rho U_w}^2}, \quad \boldsymbol{Nu} = \frac{\boldsymbol{x q_w}}{\boldsymbol{k(T_w - T_\infty)}}, \quad \boldsymbol{Sh} = \frac{\boldsymbol{x q_m}}{\boldsymbol{D_B(c_w - c_\infty)}} \tag{16}$$

Where $\boldsymbol{\tau_w}$ is the local wall shear stress, $\boldsymbol{q_w}$ is the local heat flux and $\boldsymbol{q_m}$ is the mass flux which can be determined as

$$\boldsymbol{\tau_w} = \boldsymbol{\mu}\left(\frac{\partial \boldsymbol{u}}{\partial \boldsymbol{y}} + \frac{\boldsymbol{\Gamma}}{\sqrt{2}}\left(\frac{\partial \boldsymbol{u}}{\partial \boldsymbol{y}}\right)^2\right)\Bigg|_{\boldsymbol{y=0}}, \quad \boldsymbol{q_w} = -\boldsymbol{k}\frac{\partial \boldsymbol{T}}{\partial \boldsymbol{y}}\bigg|_{\boldsymbol{y=0}}, \; \boldsymbol{q_m} = -\boldsymbol{D_B}\frac{\partial \boldsymbol{C}}{\partial \boldsymbol{y}}\bigg|_{\boldsymbol{y=0}} \tag{17}$$

Using similarity transformations and equations (16), and (17), the following terms are obtained:

$$\left.\begin{aligned} (\boldsymbol{2Re_x})^{1/2}\boldsymbol{C_f} &= \left(\boldsymbol{f}''(\eta) + \frac{\boldsymbol{\lambda}}{\boldsymbol{2}}(\boldsymbol{f}''(\eta))^2\right)_{\eta=\boldsymbol{0}} \\ \boldsymbol{e}^{-x/2l}(\boldsymbol{2Re_x})^{-1/2}\boldsymbol{Nu} &= -\Theta'(\boldsymbol{0}) \\ \boldsymbol{e}^{-x/2l}(\boldsymbol{Re_x})^{-1/2}\boldsymbol{Sh} &= -\boldsymbol{\phi}'(\boldsymbol{0}) \end{aligned}\right\} \tag{18}$$

III. Solution Algorithm:

We utilise the MATLAB software package's built-in solver named bvp4c function to solve boundary value problems (10) – (12) with boundary conditions (13) and (14). The algorithm is based on reducing the nonlinear ordinary differential equations (10) – (12) into a system of first order nonlinear differential equations with boundary conditions (13) and (14) as follows.

$$\boldsymbol{f} = \boldsymbol{y_1}, \boldsymbol{f}' = \boldsymbol{y_2}, \boldsymbol{f}'' = \boldsymbol{y_3}, \Theta = \boldsymbol{y_4}, \Theta' = \boldsymbol{y_5}, \boldsymbol{\phi} = \boldsymbol{y_6}, \boldsymbol{\phi}' = \boldsymbol{y_7} \tag{19}$$

Using similarity transformation, equations (10) - (12) reduce to first order ordinary differential equations

$$\boldsymbol{y_1}' = \boldsymbol{y_2} \tag{20}$$

$$\boldsymbol{y_2}' = \boldsymbol{y_3} \tag{21}$$

$$\boldsymbol{y_3}' = \frac{\boldsymbol{1}}{(1 + \lambda y_3)}[\boldsymbol{2y_2}^2 - \boldsymbol{y_1 y_3} + (\boldsymbol{K} + \boldsymbol{M})\boldsymbol{y_2}] \tag{22}$$

$$\boldsymbol{y_4}' = \boldsymbol{y_5} \tag{23}$$

$$\boldsymbol{y_5}' = \frac{\boldsymbol{Pr}}{(1 + Nr)}[\boldsymbol{y_2 y_4} - \boldsymbol{y_1 y_5} - \boldsymbol{2Q y_4} - \boldsymbol{N_b y_5 y_7} - \boldsymbol{N_t y_5}^2] \tag{24}$$

$$y_6{}' = y_7 \tag{25}$$

$$y_7{}' = -LePry_1y_7 - \frac{N_t}{N_b}\left[\frac{Pr}{1+Nr}\left(y_2y_4 - y_1y_5 - 2Qy_4 - N_by_5y_7 - N_ty_5{}^2\right)\right] \tag{26}$$

The boundary conditions yield

$$\left.\begin{array}{ll} y_1(0) = 0,\ y_2(0) = 1,\ y_4(0) = 1,\ y_6(0) = 1 & at\ \eta = 0 \\ y_2(\eta) \to 0,\ y_4(\eta) \to 0,\ y_6(\eta) \to 0 & at\ \eta \to \infty \end{array}\right\} \tag{27}$$

IV. Results and discussion:

The objective of the present paper is to study the rate of heat and mass transfer in MHD Williamson nanofluid flow through porous medium over an exponentially stretching sheet subject to the thermal radiation and heat generation/absorption. In this section, a brief study of the effect of various parameters like Brownian motion parameter, Thermophoresis parameter, Thermal radiation parameter, Prandtl number, Heat source/sink parameter, Williamson parameter, Porosity parameter, Hartmann number and Lewis number on hydromagnetic Williamson nanofluids flow over an exponentially stretching sheet in porous medium is to be discussed. Additionally mentioned are the effects of skin friction coefficient, Nusselt number and Sherwood number for various values of parameter. The behaviour of velocity profile, temperature profile and concentration profile can be found with the variation of several parameters of Williamson nanofluids. The MATLAB function bvp4c is used to solve the system of ODEs generated by equations (10) to (12) and (18).

Figure 1. shows that under $\boldsymbol{\lambda = 0.5, k = 1.5, Nr = 0.2, Pr = 1.5, Q = 1, N_b = 1, N_t = 1, Le = 1}$ on increasing Hartmann number, the velocity of the fluid decreases implying that near stretching sheet velocity seems to settle down on increasing magnetic field. For the decrease in velocity the retarding force is responsible.

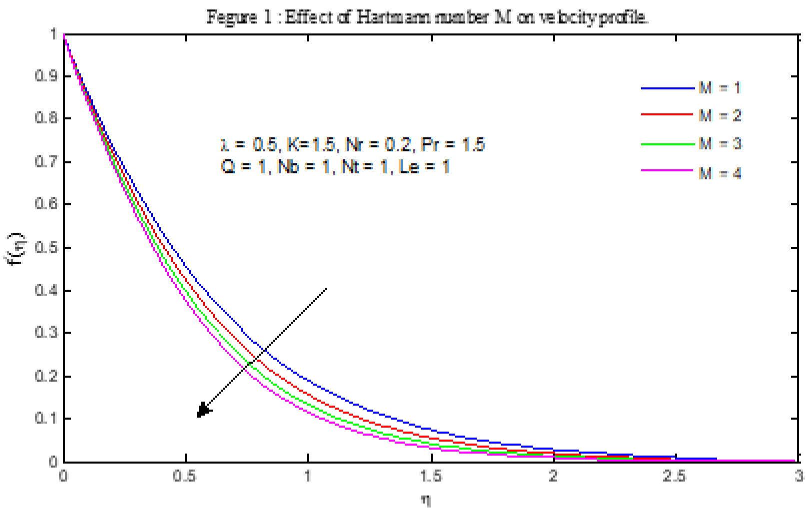

Figure 2. depict the impact of Williamson parameter on velocity profile. It appears that $\boldsymbol{f'}(\eta)$ boosts with the ever-increasing values of Williamson type parameter, whereas the rest of the parameters are chosen to be unvarying. Figure 3 is the plot of velocity of the fluid for various values of porosity parameter. It is clearly observed from this figure that as the porosity parameter $\boldsymbol{k}$ increases, the velocity profile decreases, whereas the rest of the parameters are chosen to be unvarying.

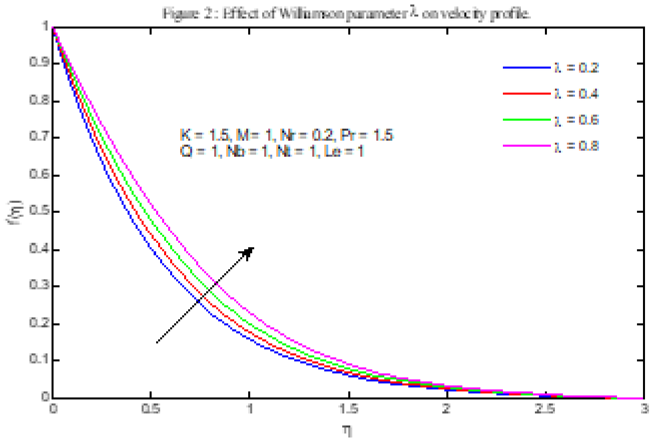

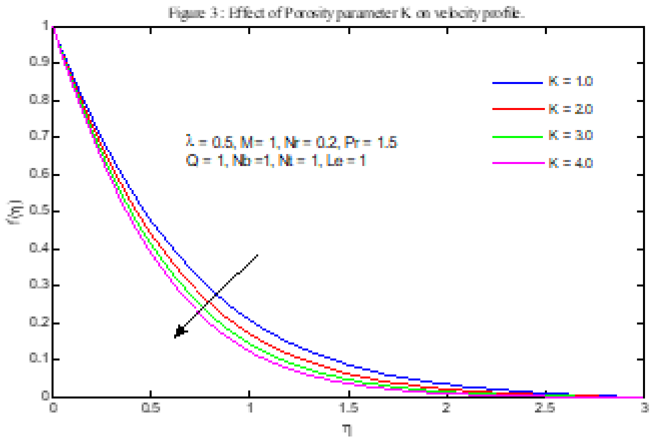

Figure 4 illustrates the impact of the thermal radiation parameter on the temperature profile. It demonstrates that the temperature profile rises on increasing thermal Radiation parameter. The relationship between Prandtl number and temperature profile is shown in the Figure 5. It explores that the temperature profile increases with an escalation in the values of Prandtl number. For higher values of heat source/sink parameter $\boldsymbol{Q}$, the temperature shows an increasing behaviour as can be seen in Figure 6. Figure 7 depicts the effect of Brownian motion parameter $\boldsymbol{N_b}$ on temperature profile. It is depicted that there is rise in temperature profile by increasing the Brownian motion parameter $\boldsymbol{N_b}$ implies that the thermal boundary layer is also increased. To observe the characteristics of temperature distribution $\Theta(\eta)$ under the influence of various values of thermophoresis parameter $\boldsymbol{N_t}$ as determined in Figure 8. It is noted that increase the value of thermophoresis parameter $\boldsymbol{N_t}$ causes the reduction in temperature profile.

Figure 4 : Effect of Thermal radiation parameter Nr on temperature profile.

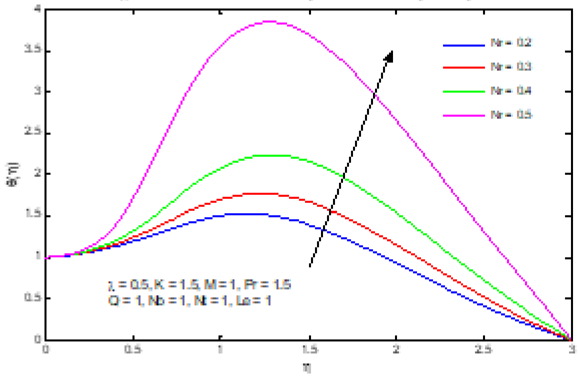

Figure 5 : Effect of Prandtl number Pr on temperature profile.

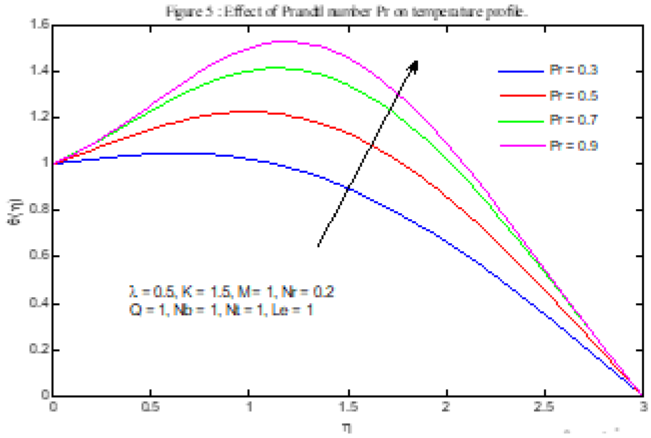

Figure 6 : Effect of Heat source/sink parameter Q on temperature profile.

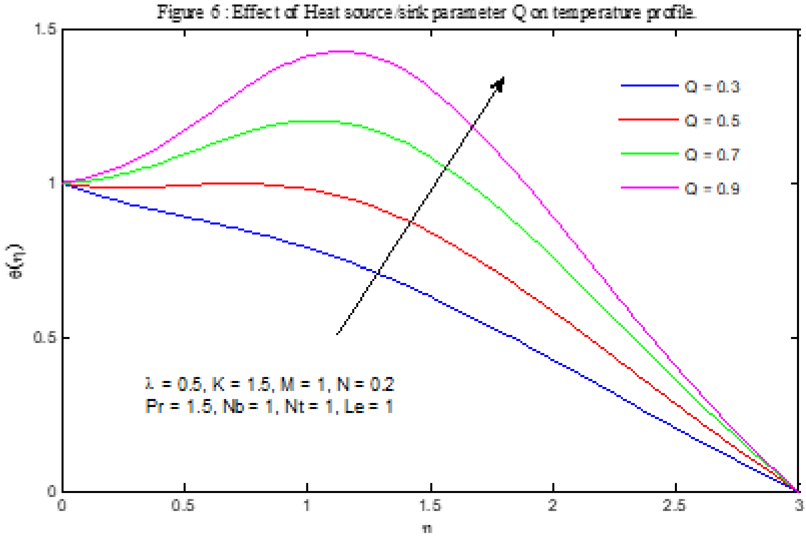

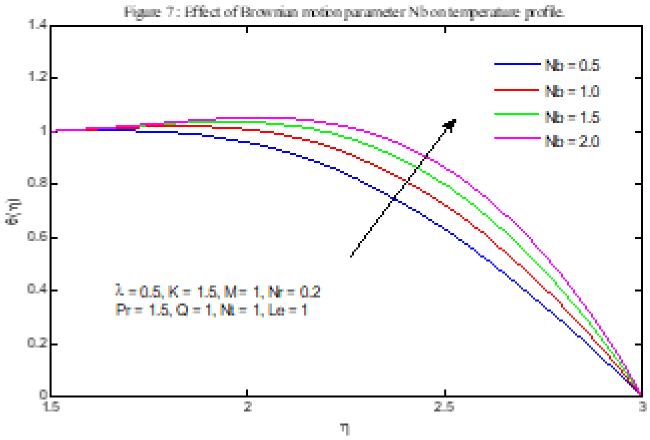

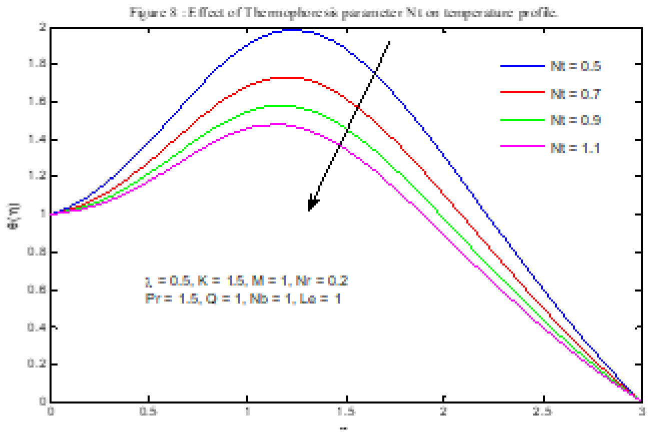

Figure 9. depict the effect of Lewis number Le on concentration profile. This figure shows that irregular oscillation is obtained on increasing Lewis number Le versus η by fixing λ = 0.5, K = 1.5, M = 1, Nr = 0.2, Pr = 1.5, Q = 1, $\boldsymbol{N_b}$ = 1, $\boldsymbol{N_t}$ = 1. To observe the characteristics of concentration profile $\boldsymbol{\phi}$(η) under the influence of various values of Prandtl number Pr as determined in Figure 10. It shows that increase the value of parameter Pr causes the reduction in concentration profile $\boldsymbol{\phi}$(η) for fixed values of λ = 0.5, K = 1.5, M = 1, Nr = 0.2, Q = 1, $\boldsymbol{N_b}$ = 1, $\boldsymbol{N_t}$ = 1, Le = 1. Figure 11 illustrates the influence of Brownian motion parameter $\boldsymbol{N_b}$ on concentration function $\boldsymbol{\phi}$(η). It demonstrates that the concentration profile $\boldsymbol{\phi}$(η) rises as the Brownian motion parameter $\boldsymbol{N_b}$ rises versus η by fixing λ = 0.5, K = 1.5, M = 1, Nr = 0.2, Pr = 1.5, Q = 1, $\boldsymbol{N_t}$ = 1, Le = 1. The direct relationship between thermophoresis parameter $\boldsymbol{N_t}$ and concentration function $\boldsymbol{\phi}$(η) as shown in figure 12. It demonstrates that the concentration profile decreases with an escalation in the values of thermophoresis parameter $\boldsymbol{N_t}$ whereas the rest of the parameters are chosen to be unvarying.

Figure 9 : Effect of Lewis number Le on Concentration profile.

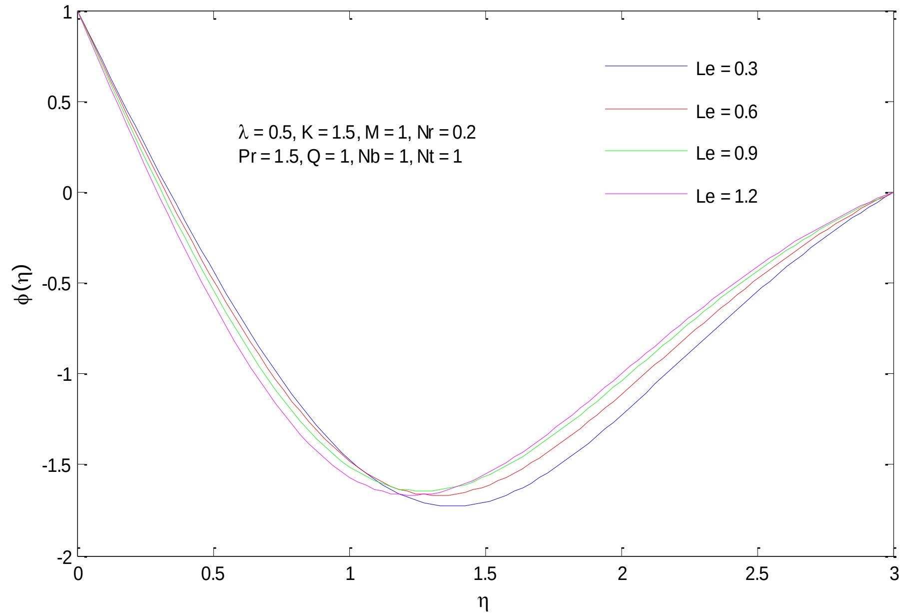

Figure 10 : Effect of Prandtl number Pr on Concentration profile.

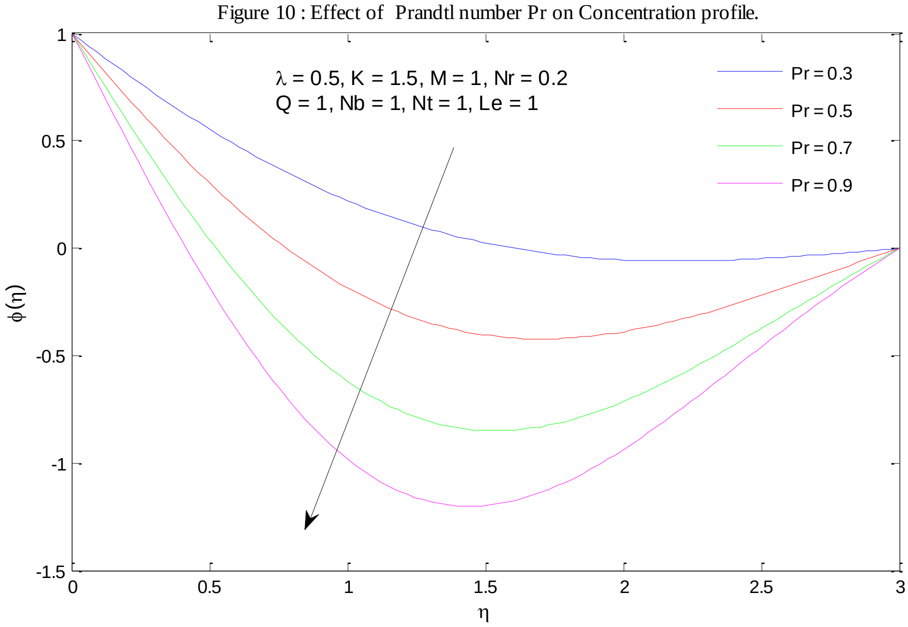

Figure 11 : Effect of Brownian motion parameter Nb on Concentration profile.

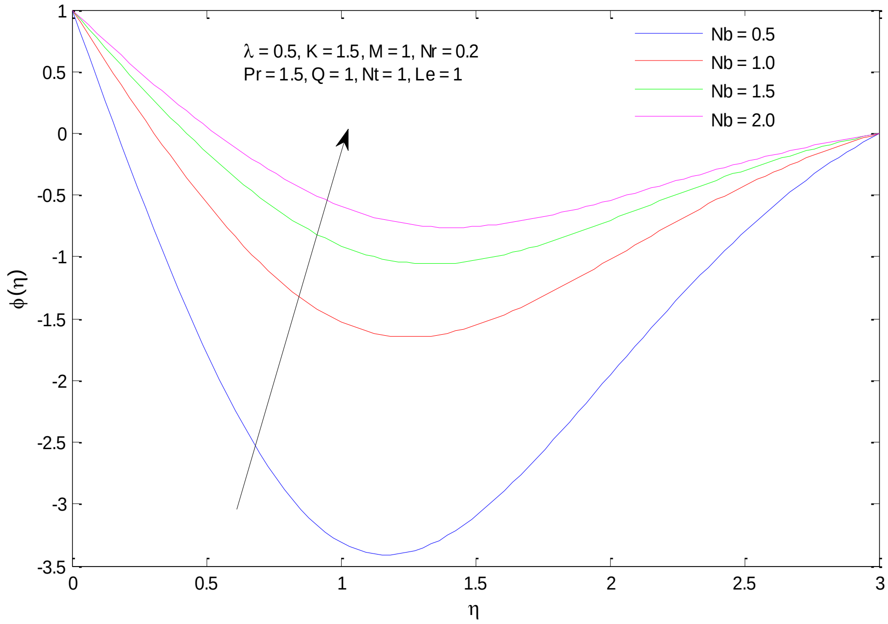

Figure 12 : Effect of Thermophoresis parameter Nt on Concentration profile.

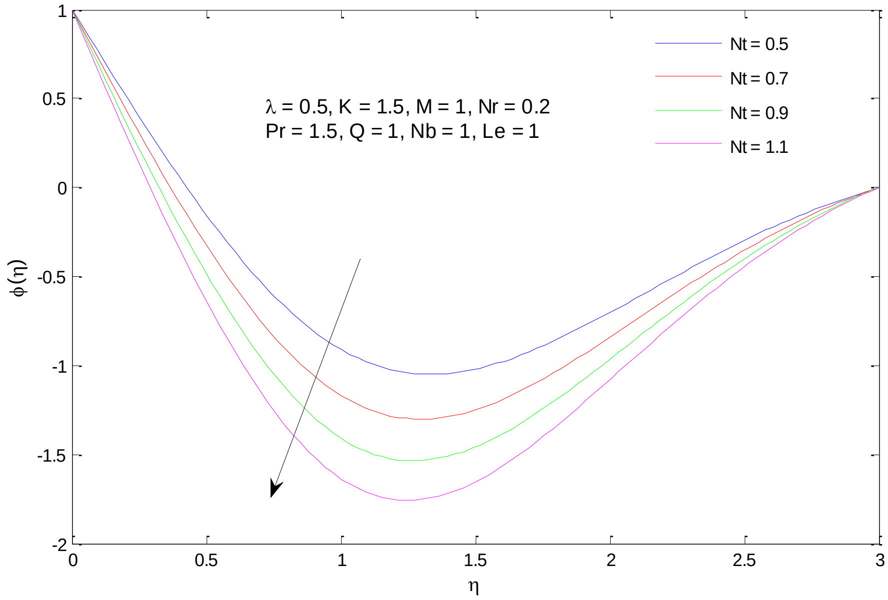

Table 1 portrays the effect of Williamson parameter, porosity parameter and Hartmann number on skin friction coefficient. Table 1 show that an escalation in Williamson parameter results in the decline of the skin friction coefficient. As we increase the porosity parameter and Hartmann number, the skin friction coefficient also increases.

Variation of temperature gradient and nanoparticle volume friction gradient with respect to Williamson parameter, porosity parameter, Hartmann number, Thermal radiation parameter, Prandtl number, Heat source/sink parameter, Brownian motion parameter and thermophoresis parameter are presented in Table 2. From this table, we can see that $-\Theta'(\mathbf{0})$ increase with increasing values of thermophoresis parameter, Williamson parameter and Brownian motion parameter and $-\boldsymbol{\phi}'(\mathbf{0})$ increase with increasing values of porosity parameter, Hartmann number, thermal radiation parameter, Prandtl number, Heat source/sink parameter and thermophoresis parameter. For higher values of porosity parameter, Hartmann number, thermal radiation parameter, Prandtl number, heat source/sink parameter, the wall temperature gradient shows decreasing a behaviour and for higher values of Williamson parameter, Brownian motion parameter, $-\boldsymbol{\phi}'(\mathbf{0})$ shows a decreasing behaviour.

Table 1: Effects of various parameters on C_f.

λ	K	M	$-f''(0)$	$-\left(f''(0)+\frac{\lambda}{2}(f''(0))^2\right)$
0	1.5	1	2.0395	**2.0395**
0.5	1.5	1	1.4171	**1.9191**
1.0	1.5	1	0.9538	**1.4087**
0.5	**0**	1	1.2255	**1.6010**
0.5	**0.5**	1	1.2988	**1.7205**
0.5	**1**	1	1.3619	**1.8256**
0.5	1.5	**0**	1.2988	**1.7205**
0.5	1.5	**0.5**	1.3619	**1.8256**
0.5	1.5	**1**	1.4171	**1.9191**

Table 2: Effects of various parameters on Sherwood number and Nusselt number.

λ	K	M	Nr	Pr	Q	N_b	N_t	$-\theta'(0)$	$-\phi'(0)$
0.2	1.5	1	0.2	1.5	1	1	1	**- 0.1515**	**3.5282**
0.5	1.5	1	0.2	1.5	1	1	1	**- 0.1427**	**3.4412**
0.8	1.5	1	0.2	1.5	1	1	1	**- 0.1323**	**3.3156**
0.5	**0**	1	0.2	1.5	1	1	1	**- 0.1356**	**3.2027**
0.5	**0.5**	1	0.2	1.5	1	1	1	**- 0.1392**	**3.3010**
0.5	**1**	1	0.2	1.5	1	1	1	**- 0.1414**	**3.3788**
0.5	1.5	**0**	0.2	1.5	1	1	1	**- 0.1392**	**3.3010**
0.5	1.5	**0.5**	0.2	1.5	1	1	1	**- 0.1414**	**3.3788**
0.5	1.5	**1**	0.2	1.5	1	1	1	**- 0.1427**	**3.4412**
0.5	1.5	1	**0.1**	1.5	1	1	1	**- 0.1297**	**3.4640**
0.5	1.5	1	**0.3**	1.5	1	1	1	**- 0.1532**	**3.5133**
0.5	1.5	1	**0.4**	1.5	1	1	1	**- 0.1570**	**3.7915**
0.5	1.5	1	0.2	**0**	1	1	1	**0.1832**	**0.3333**
0.5	1.5	1	0.2	**0.5**	1	1	1	**- 0.2863**	**1.5244**
0.5	1.5	1	0.2	**1**	1	1	1	**- 0.3080**	**2.7240**
0.5	1.5	1	0.2	1.5	**0**	1	1	**0.5807**	**0.4144**
0.5	1.5	1	0.2	1.5	**0.5**	1	1	**0.1084**	**1.2864**
0.5	1.5	1	0.2	1.5	**1**	1	1	**- 0.1427**	**2.7240**
0.5	1.5	1	0.2	1.5	1	**0.5**	1	**- 0.1944**	**4.8419**
0.5	1.5	1	0.2	1.5	1	**1**	1	**- 0.1427**	**2.7240**
0.5	1.5	1	0.2	1.5	1	**1.5**	1	**- 0.1050**	**-3.6972**
0.5	1.5	1	0.2	1.5	1	1	**0.2**	**- 0.9927**	**1.7735**
0.5	1.5	1	0.2	1.5	1	1	**0.5**	**- 0.3712**	**1.8568**
0.5	1.5	1	0.2	1.5	1	1	**1**	**- 0.1427**	**2.7240**

V. Conclusions:

In this analysis we have presented heat transfer attributes of Williamson type fluid flows via an exponentially stretching sheet in the porous medium are studied under the influence of heat generation/absorption and thermal radiation. On the Navier-Stokes theory, the governing partial differential equations are based. The main points are listed below:

- Velocity profile settles at higher values for increasing Williamson parameter, whereas it settles at lower values for increasing Hartmann number and porosity parameter.
- Concentration profile is declining function of Prandtl number and thermophoresis parameter while Brownian motion parameter enhances the concentration profile. The concentration profile has irregular oscillation behaviour with increases Lewis number.
- Temperature profile elevates on increasing thermal radiation parameter, Prandtl number, heat source/sink parameter and Brownian motion parameter whereas it drops down for higher values of thermophoresis parameter.
- Skin friction coefficient reduces by raising the value of Williamson parameter whereas it increases on increasing porosity parameter and Hartmann number.

- Wall temperature gradient increases for higher values of Williamson parameter, Brownian motion parameter, thermophoresis parameter and decreases for higher values of porosity parameter, Hartmann number, thermal radiation parameter, Prandtl number, heat source/sink parameter.
- Sherwood number shows direct relation with porosity parameter Hartmann number, thermal radiation parameter, Prandtl number, heat source/sink parameter, thermophoresis parameter and opposite relation with Williamson parameter, Brownian motion parameter.

References:

[1]. Sakiadis, B.C. (1961). Boundary layer behaviour on continuous solid flat surfaces American Institute of Chemical Engineers Journal, 7, 26-28.
[2]. Tsou, F.K., Sparrow, E.M., Goldstein, R.J. (1967). Flow and heat transfer in the boundary layer on a continuous moving surface., 10(2), 219–235.
[3]. Erickson, L.E., Fan, L.T., Fox, V.G. (1966). Heat and mass transfer in the laminar boundary layer flow of a moving flat surface with constant surface velocity and temperature focusing on the effects of suction/injection Ind. Eng. Chem. Fundam., 5, 19-2.
[4]. Khan, M.R., (2020). Numerical analysis of oblique stagnation point flow of nanofluid over a curved stretching/shrinking surface, Phys. Scripta, 95 (10), 105704.
[5]. Li, X., Khan, A.U., Khan, M.R., Nadeem, S. & Khan, S.U. (2019). Oblique stagnation point flow of nanofluids over stretching/shrinking sheet with Cattaneo–Christov heat flux model: existence of dual solution, Symmetry, 11 (9), 1070.
[6]. Khan, M.R., Li, M., Mao, S., Ali, R.& Khan, S. (2021). Comparative study on heat transfer and friction drags in the flow of various hybrid nanofluids effected by aligned magnetic field and nonlinear radiation, Sci. Rep., 11 (1), 1-14.
[7]. Bachok, N., Ishak, A. & Pop, I. (2010). Boundary-layer flow of nanofluids over a moving surface in a flowing fluid, 49(9), 1663–1668.
[8]. Khan, M. R., Pan, K., Khan, A. U. & Nadeem, S. (2020). hybrid nanofluid near the stagnation point flow over a curved surface., Physica A: Statistical Mechanics and its Applications, 123959.
[9]. Nadeem, S. & Khan A.U. (2019). MHD oblique stagnation point flow of nanofluid over an oscillatory stretching/shrinking sheet: existence of dual solutions, Phys. Scripta, 94 (7), 075204.
[10]. Choi S. (1995). Enhancing thermal conductivity of fluids with nanoparticle. in: Siginer D.A., Wang H.P.(Eds.), Developments and Applications of Non- Newtonian Flows, Siginer D.A. and Wang H.P., eds, MD-vol. 231/FED378 vol. 66, ASME, New York, 99–105.
[11]. Buongiorno, J. (2006). Convective transport in nanofluids, J. Heat Transf., 128, 240 - 250.
[12]. Nield, D. & Kuznetsov, A. (2013). The Cheng-Minkowycz problem for natural convective boundary layer flow in a porous medium saturated by a nanofluid: a revised model, Int. J. Heat Mass Transf., 65, 682-685.
[13]. Pal, D. & Mandal, G. (2015). Hydromagnetic convective–radiative boundary layer flow of nanofluids induced by a non-linear vertical stretching/shrinking sheet with viscous–Ohmic dissipation., Powder Technology, 279, 61–74.
[14]. Das, K. (2015). Nanofluid flow over a non-linear permeable stretching sheet with partial slip., J. Egypt. Math. Soc., 23, 451-456.
[15]. Ali, N., Ullah Khan, S., Sajid, M., & Abbas, Z. (2016). MHD flow and heat transfer of couple stress fluid over an oscillatory stretching sheet with heat source/sink in porous medium. Alexandria Engineering Journal, 55(2), 915–924.
[16]. Bhatti, M.M. & Rashidi M.M. (2016). Entropy generation with nonlinear thermal radiation in MHD boundary layer flow over a permeable shrinking/stretching sheet numerical solution. journal of nanofluids, 5 (4), 543-548.
[17]. Williamson, R.V. (1929). The flow of pseudoplastic materials. Ind. Eng. Chem., 21, 1108-1111.
[18]. Kumar, K. A., Reddy, J. V., Sugunamma, V. & Sandeep, N. (2019). Simultaneous solutions for MHD flow of Williamson fluid over a curved sheet with non-uniform Heat sorce/sink. Heat Transfer Research, 50(6), 581–603.
[19]. Malik, M. Y., Salahuddin, T., Hussain, A., Bilal, S. & Awais, M. (2015). Homogeneous-heterogeneous reactions in Williamson fluid model over a stretching cylinder by using Keller box method. AIP Advances, 5(10), 107227.
[20]. Ahmed, K., Khan, W.A., Akbar, T., Rasool, G., Alharbi, S.O. & Khan, I. (2021). Numerical investigation of mixed convective Williamson fluid flow over an exponentially stretching permeable curved surface. Fluids, 6 (7), 260.
[21]. Krishnamurthy, M.R., Prasannakumara, B.C., Gireesha, B.J. & Gorla, R.S. (2016). Effect of chemical reaction on MHD boundary layer flow and melting heat transfer of Williamson nanofluid in porous medium. Engineering Science and Technology, an International Journal, 19, 53-61.
[22]. Nadeem, S., Hussain, S. T. & Lee, C., (2013). Flow of a Williamson fluid over a stretching sheet Braz. J. Chem. Eng. 30 (3), 619–625.
[23]. Nadeem, S. & Hussain, S.T. (2014). Heat transfer analysis of Williamson fluid over exponentially stretching surface, Appl. Math. Mech. Engl. Ed., 35 (4), 489–502.
[24]. Hayat, T., Khalid, U. & Qasim, M. (2012). Steady flow of a Williamson fluid past a porous plate., 7(2), 302–306.
[25]. Nadeem, S. & Hussain, S.T. (2014). Flow and heat transfer analysis of Williamson nanofluid, Appl. Nanosci. 4, 1005–1012.
[26]. Ahmed, K. & Akbar, T. (2021). Numerical investigation of magnetohydrodynamics Williamson nanofluid flow over an exponentially stretching surface. Advances in Mechanical Engineering, 13(5),1 –12.
[27]. Srinivasulu, T., Goud, B. S. (2021). Effect of inclined magnetic field on flow, heat and mass transfer of Williamson nanofluid over a stretching sheet. Case Studies in Thermal Engineering, 23, 100819.
[28]. Yahya, A. U., Salamat, N., Habib, D., Ali, B., Hussain, S., & Abdal, S. (2021). Implication of Bio-convection and Cattaneo-Christov heat flux on Williamson Sutterby nanofluid transportation caused by a stretching surface with convective boundary. Chinese Journal of Physics, 73, 706–718.
[29]. Zhang, X., Yang, D., Rehman, M. I., Mousa, A. A. & Hamid, A. (2022). Numerical simulation of bioconvection radiative flow of Williamson nanofluid past a vertical stretching cylinder with activation energy and swimming microorganisms. Case studies in thermal engineering, 33, 101977.
[30]. Amjad, M., Ahmed, K., Akbar, T., Muhammad, T., Ahmed, I. & Alshomrani, A. S. (2022). Numerical investigation of double diffusion heat flux model in Williamson nanofluid over an exponentially stretching surface with variable thermal conductivity. Case Studies in Thermal Engineering, 36, 102231.
[31]. Jalili, B., Ganji, A. D., Jalili, P., Nourazar, S. S. & Ganji, D. D. (2022). Thermal analysis of Williamson fluid flow with Lorentz force on the stretching plate. Case Studies in Thermal Engineering, 39, 102374.

[32]. Yousef, N. S., Megahed, A. M., Ghoneim, N. I., Elsafi, M. E. & Fares, E. (2022). Chemical reaction impact on MHD dissipative Casson-williamson nanofluid flow over a slippery stretching sheet through porous medium. Alexandria Engineering journal, 61(12), 10161-10170.

[33]. Shafiq, A., Çolak, A. B., Sindhu, T. N., Al-Mdallal, Q. M. & Abdeljawad, T. (2021). Estimation of unsteady hydromagnetic Williamson fluid flow in a radiative surface through numerical and artificial neural network modeling. Scientific Reports, 11(1), 14509.

[34]. Hamid, A., Hashim, Alghamdi, M., Khan, M. & Alshomrani, A.S. (2019). An investigation of thermal and solutal stratification effects on mixed convection flow and heat transfer of Williamson nanofluid. Journal of Molecular Liquids, 284, 307-315.

[35]. Ramzan, M., Rehman, S., Junaid, M. S., Saeed, A., Kumam, P. & Watthayu, W. (2022). Dynamics of Williamson Ferro-nanofluid due to bioconvection in the portfolio of magnetic dipole and activation energy over stretching sheet. International communications in Heat and Mass transfer, 137, 106245.

[36]. Ogunseye, H. A., Salawu, S. O. & Fatunmbi, E. O. (2021). A numerical study of MHD heat and mass transfer of a reactive Casson-Williamson nanofluid past a vertical moving cylinder, partial differential equations in applied mathematics, 4, 100148.

[37]. Nawaz, M. & Sadiq, M. A. (2021). Unsteady heat transfer enhancement in Williamson fluid in Darcy-Forchheimer porous medium under non-Fourier condition of heat flux case studies in thermal engineering, 28, 101647.

[38]. Kumar, A.; Tripathi, R.; Singh, R.; Chaurasiya, V.K. (2020). Simultaneous effects of nonlinear thermal radiation and Joule heating on the flow of Williamson nanofluid with entropy generation. Physica A: Statistical Mechanics and its Applications, 123972.

[39]. Song, Y., Hamid, A., Sun, T., Ijaz Khan, M., Qayyum, S., & Naveen Kumar, R. et al. (2022). Unsteady mixed convection flow of magneto-Williamson nanofluid due to stretched cylinder with significant non-uniform heat source/sink features. Alexandria Engineering Journal, 61(1), 195-206.